Creation and destruction of magnetic fields

Matthias Rempel

January 16, 2019

1 Introduction - Magnetic fields in the universe

Objects in the universe from scales of a planet to the size of a galaxy show evidence for large-scale magnetic fields. Despite the fact that the physical conditions in these objects are quite different, the creation and destruction of magnetic fields is closely linked to turbulent motions of a highly conducting fluid within these bodies. Dynamo theory focuses on a characterization of conditions under which a flow of highly conducting fluid can sustain a magnetic field against resistive decay. This chapter is an introduction to dynamo theory with primary focus on general concepts rather than detailed applications; the latter are discussed in Volume III of this series. We start this introduction with a brief overview of the properties of objects with large-scale magnetic fields in the universe.

1.1 Earth and other planets

The magnetic field of the Earth has a strength of about 0.5 G with mainly dipolar character. Currently the dipole axis is tilted by about 11° with respect to the axis of rotation. From studies of rock magnetism (when rocks cool below the Curie point they preserve the magnetic field that was present in them at that time) it is known that the Earth had a magnetic field over the past 3.5×10^9 years and that the strength and orientation of the field varied significantly on time scales of 10^3 to 10^4 years. A given polarity typically dominates for about 200 000 years with quick reversals on a time scale of a few thousand years in between. While the orientation of the axis of the dipole changes significantly with time, the dipole moment is aligned with the axis of rotation when averaged over $\sim 10^4$ years.

Currently, the Moon does not have a large-scale magnetic field, but there are indications from lunar rocks that the Moon had a large-scale field more than 3×10^9 years ago. Of the other terrestrial planets only Mercury shows a large-scale field. All the gas giants (Jupiter, Saturn, Uranus and Neptune) show a magnetic field of significant strength (cf. Ch. **??**, Table **??**, and, *e.g.*, Fig. **??**). Both Uranus and Neptune have a dipole axis significantly tilted to the rotation axis (indicating a different mode of the dynamo), while Saturn is

the planet with the most axisymmetric field. Also Ganymede, a large satellite of Jupiter, has a large-scale magnetic field.

While in terrestrial planets and the moons of the Jupiter system liquid iron cores are responsible for the dynamo action, the gas giants Jupiter and Saturn have inner regions of metallic hydrogen (formed under high pressure) with a conductivity similar to that of molten iron. For Uranus and Neptune the detailed mixture of the conducting layer responsible for dynamo action is not well known.

1.2 Sun and other stars

Magnetic fields on the Sun are measured primarily through the Zeeman effect. While it is in most cases difficult to observe the actual splitting of the spectral lines, most measurements make use of the linear and circular polarization resulting from the presence of a magnetic field. The Sun shows magnetic field on all observable scales with a significant range in field strength, from individual sunspots with magnetic field strengths of 2 500 to 3 000 G to the average field strength of the global field of only a few Gauss.

The most prominent feature of solar magnetism is the 11 year sunspot cycle (if one considers the field reversals the real period is 22 years), which is reflected in the changing number of sunspots appearing on the surface of the Sun. In the beginning of a cycle spots appear at latitudes of about 35°, while close to the end they appear almost at the equator. This property is commonly summarized in the so-called solar butterfly diagram. During the epoch of minimum, the large-scale field of the Sun is most dipolar; the reversal of the poles takes place during solar maximum. On the longer time scale the magnetic activity changes significantly in amplitude and is interrupted by epochs of $100 - 200$ years in duration where sunspots are completely absent. Over time scales beyond the direct observation records the magnetic behavior of the Sun can be derived from the concentration of cosmogenic isotopes in tree-rings (^{14}C) and ice cores (^{14}C and ^{10}Be), allowing for a reconstruction of solar activity over the last 300 000 years. Over these time scales the Sun exhibits a behavior similar to that in recent decades, namely a dominant 11 year sunspot cycle interrupted by epochs of sustained low activity. For more details on the solar magnetic field we refer to the text book of Stix (2004).

Magnetic activity is common among other solar-like stars (stars with an outer convection zone and a radiative interior). Observations of the stellar luminosity or of chromospheric (UV/optical) and coronal (X-ray) emission show that a majority of solar-like stars are magnetically active and around a third to a half show cyclic activity with periods in the range from 3 to 30 years (e.g., Schrijver & Zwaan (2000)).

1.3 Galaxies

Galactic magnetic fields are measured through the polarization of radio synchrotron emissions. The magnetic field strength of galactic fields is of the order of a few μG and galaxies of almost all structures and ages exhibit a magnetic

field. The field typically shows features reflecting the structure of the matter distribution of a galaxy (e.g. spiral galaxies have spiral magnetic fields).

Galactic magnetic fields are of particular interest for dynamo theorists, since galaxies are the only objects in the universe in which the dynamo region is directly accessible through observation.

2 Magnetohydrodynamics

The mathematical basis for dynamo theory is magnetohydrodynamics (MHD). Since most of the derivations in this chapter are focused around the induction equation we will discuss only the induction equation in greater detail and refer to textbooks for a detailed discussion of MHD ((Parker 1979), (Shu 1992), (Davidson 2001), (Parker 2007)). Here we only summarize the most important equations for later reference.

2.1 MHD equations

The general assumptions underlying the MHD approach are the validity of the continuum approximation, non-relativistic motions, and quasi-neutrality of the plasma. It is further assumed that the collisional coupling between different ions constituting the plasma is sufficiently strong to treat the plasma as a single fluid (e.g., same temperature for all ions).

The full set of MHD equations combines the induction equation with the Navier-Stokes equations including the Lorentz-force $\mathbf{j}\times\mathbf{B}$, resulting in equations for continuity, force balance, energy conservation, and magnetic field, respectively:

$$\frac{\partial \varrho}{\partial t} = -\boldsymbol{\nabla}\cdot(\varrho \boldsymbol{v}) \tag{1}$$

$$\varrho\frac{\partial \boldsymbol{v}}{\partial t} = -\varrho(\boldsymbol{v}\cdot\boldsymbol{\nabla})\boldsymbol{v} - \boldsymbol{\nabla}p + \varrho\boldsymbol{g} + \frac{1}{\mu_0}(\boldsymbol{\nabla}\times\boldsymbol{B})\times\boldsymbol{B} + \boldsymbol{\nabla}\cdot\boldsymbol{\tau} \tag{2}$$

$$\varrho\frac{\partial e}{\partial t} = -\varrho(\boldsymbol{v}\cdot\boldsymbol{\nabla})e - p\boldsymbol{\nabla}\cdot\boldsymbol{v} + \boldsymbol{\nabla}\cdot(\kappa\boldsymbol{\nabla}T) + Q_\nu + Q_\eta \tag{3}$$

$$\frac{\partial \boldsymbol{B}}{\partial t} = \boldsymbol{\nabla}\times(\boldsymbol{v}\times\boldsymbol{B} - \eta\,\boldsymbol{\nabla}\times\boldsymbol{B})\ . \tag{4}$$

Here $\boldsymbol{v}$ denotes fluid velocity, $\boldsymbol{B}$ magnetic field, e specific internal energy, p gas pressure, ϱ mass density, $\boldsymbol{g}$ gravity, τ viscous stress tensor, and Q_ν viscous heating given by

$$Q_\nu = \tau_{ik}\Lambda_{ik}\ , \tag{5}$$

with the deformation tensor $\boldsymbol{\Lambda}$

$$\Lambda_{ik} = \frac{1}{2}\left(\frac{\partial v_i}{\partial x_k} + \frac{\partial v_k}{\partial x_i}\right), \tag{6}$$

and the viscous stress tensor τ

$$\tau_{ik} = 2\varrho\nu\left(\Lambda_{ik} - \frac{1}{3}\delta_{ik}\boldsymbol{\nabla}\cdot\boldsymbol{v}\right). \tag{7}$$

The resistive (Ohmic) dissipation Q_η is given by

$$Q_\eta = \frac{\eta}{\mu_0}(\boldsymbol{\nabla}\times\boldsymbol{B})^2\ . \tag{8}$$

The pressure p can be computed from the internal energy e through the equation of state

$$p = (\gamma - 1)\,\varrho\, e\ . \tag{9}$$

Here ν, η and κ are the values of the viscosity, magnetic diffusivity, and thermal conductivity; μ_0 denotes the permeability of the vacuum.

As an aside here, we point out one property of magnetic fields that guides our thinking about its effects in the force balance of Eq. (2): using a vector formula, the Lorentz force can be shown to equal:

$$\frac{1}{\mu_0}(\boldsymbol{\nabla}\times\boldsymbol{B})\times\boldsymbol{B} = -\nabla\frac{B^2}{2\mu_0} + \frac{1}{\mu_0}(\boldsymbol{B}\cdot\boldsymbol{\nabla})\boldsymbol{B}, \tag{10}$$

which shows that the Lorentz force is a sum of an isotropic pressure-like force and a tension force related to the curvature of the field. The ratio of the magnetic and gas pressure terms in Eq. (2) is commonly referred to as the plasma β:

$$\beta \equiv \frac{2\mu_0 p}{B^2}. \tag{11}$$

The natural approach to the dynamo problem would be to solve the MHD equations for a given setup with a magnetic field in order to see if the magnetic field can be maintained by the velocity field. Unfortunately this approach is currently still strongly restricted by the available computing power (at least for the case of the solar dynamo). We briefly discuss in Sect. 5.3 the current status of 3D dynamo simulations; more discussion of that topic can be found in Volume III of the series. For understanding the fundamental concepts we discuss the dynamo problem in the following sections only based on the induction equation, basically asking the question of whether a given velocity field $\boldsymbol{v}$ can sustain a magnetic field $\boldsymbol{B}$ against resistive decay. This approach is also called the kinematic approach and is valid as long as the Lorentz-force in the force equation can be neglected. The kinematic approach is very helpful to discuss the general properties a velocity field has to have in order to qualify as a dynamo, which is the main focus of this introduction to dynamo theory.

2.2 Induction equation

The induction equation arises from Ohm's law combined with the non-relativistic approximation of the Maxwell equations. In its most general form Ohm's law is

a relation between electric current, electric field, magnetic field, plasma motions and electron pressure gradients. Ohm's law is derived from an equation of motion for electrons in which the interaction with ions (defining the bulk motion of the plasma with velocity $\boldsymbol{v}$) is described through a collisional drag term:

$$n_e\, m_e \frac{d\boldsymbol{v}_e}{dt} = n_e\, q_e(\boldsymbol{E} + \boldsymbol{v}_e \times \boldsymbol{B}) - \boldsymbol{\nabla} p_e + n_e\, m_e \frac{\boldsymbol{v} - \boldsymbol{v}_e}{\tau_{ei}} \ . \tag{12}$$

Here $\boldsymbol{v}_e$ denotes the electron velocity, τ_{ei} the collision time between electrons and ions, q_e the electron charge, m_e the electron mass, n_e the electron density, and p_e the electron pressure. Using

$$\boldsymbol{j} = n_e\, q_e\, (\boldsymbol{v}_e - \boldsymbol{v}) \tag{13}$$

we can express $\boldsymbol{v}_e$ in terms of the electric current (the time derivative of $\boldsymbol{v}$ can be neglected since $m_e \ll m_i$), which leads to Ohm's law:

$$\frac{\partial \boldsymbol{j}}{\partial t} + \boldsymbol{\nabla} \cdot (\boldsymbol{v}\boldsymbol{j} + \boldsymbol{j}\boldsymbol{v}) + \frac{\boldsymbol{j}}{\tau_{ei}} = \frac{n_e q_e^2}{m_e}(\boldsymbol{E} + \boldsymbol{v} \times \boldsymbol{B}) + \frac{q_e}{m_e}\boldsymbol{j} \times \boldsymbol{B} - \frac{q_e}{m_e}\boldsymbol{\nabla} p_e \ . \tag{14}$$

Here the first two terms on the left hand side are terms related to the electron inertia; $(\boldsymbol{v}\boldsymbol{j}+\boldsymbol{j}\boldsymbol{v})$ denotes here a dyadic tensor with the components $v_n j_m + v_m j_n$; a term quadratic in $\boldsymbol{j}$ can be formally absorbed into the electron pressure). The second term on the right-hand side describes the Hall current, which becomes important if the collision time is longer than the electron gyration time, i.e., when $\tau_{ei}\, \omega_L > 1$, where $\omega_L = q_e B/m_e$ denotes the Larmor frequency. The Hall term leads to anisotropic plasma conductivity with respect to the magnetic field direction and is typically important in low density plasmas in which τ_{ei} can be very large. For stellar convection zones the Hall term, the electron pressure contribution, and the electron inertia are unimportant (unless high frequency plasma oscillations or considered), leading to the simplified Ohm's law

$$\boldsymbol{j} = \sigma(\boldsymbol{E} + \boldsymbol{v} \times \boldsymbol{B}) \tag{15}$$

with the plasma conductivity

$$\sigma = \frac{\tau_{ei} n_e q_e^2}{m_e} \ . \tag{16}$$

Using Ampere's law, $\boldsymbol{\nabla} \times \boldsymbol{B} = \mu_0 \boldsymbol{j}$, yields for the electric field in the laboratory frame

$$\boldsymbol{E} = -\boldsymbol{v} \times \boldsymbol{B} + \frac{1}{\mu_0 \sigma}\boldsymbol{\nabla} \times \boldsymbol{B} \tag{17}$$

leading to the induction equation through one of the Maxwell equations:

$$\frac{\partial \boldsymbol{B}}{\partial t} = -\boldsymbol{\nabla} \times \boldsymbol{E} = \boldsymbol{\nabla} \times (\boldsymbol{v} \times \boldsymbol{B} - \eta\, \boldsymbol{\nabla} \times \boldsymbol{B}) \tag{18}$$

with the magnetic diffusivity

$$\eta = \frac{1}{\mu_0 \sigma} \ . \tag{19}$$

In MHD the equations are typically expressed in terms of the magnetic field $\boldsymbol{B}$ and electric currents are completely eliminated from the system. This is done primarily out of mathematical convenience, since formulating the problem in terms of currents leads to intractable equations.

2.3 Advection, diffusion, and the magnetic Reynolds number

Let L be a typical length-scale and U a characteristic velocity of the problem. Expressing the time in units of L/U and the spatial derivatives in the induction equation Eq. (4) in units of L leads to the dimensionless form of the induction equation

$$\frac{\partial \boldsymbol{B}}{\partial t} = \boldsymbol{\nabla} \times \left(\boldsymbol{v} \times \boldsymbol{B} - \frac{1}{R_\mathrm{m}} \boldsymbol{\nabla} \times \boldsymbol{B} \right) \tag{20}$$

with the magnetic Reynolds number

$$R_\mathrm{m} \equiv \frac{U\,L}{\eta} \; . \tag{21}$$

The limit $R_\mathrm{m} \ll 1$ is referred to as diffusion dominated regime, in which the (dimensional) induction equation reduces to a diffusion equation equation of the form

$$\frac{\partial \boldsymbol{B}}{\partial t} = \eta \Delta \boldsymbol{B} \; . \tag{22}$$

Here we made the additional simplifying assumption of a constant magnetic diffusivity η. Assuming that the magnetic field has a typical length scale L, we can estimate from the induction equation Eq. (4) a decay time scale given by

$$\tau_\mathrm{d} \sim \frac{L^2}{\eta} \; . \tag{23}$$

The limit $R_\mathrm{m} \gg 1$ is referred to as the advection-dominated regime, in which the induction equation reduces to the equation of ideal MHD (except for possible boundary layers where diffusivity could be still important)

$$\frac{\partial \boldsymbol{B}}{\partial t} = \boldsymbol{\nabla} \times (\boldsymbol{v} \times \boldsymbol{B}) \; . \tag{24}$$

Expanding the expression of the right-hand side of this ideal induction equation leads to

$$\frac{\partial \boldsymbol{B}}{\partial t} = -(\boldsymbol{v} \cdot \boldsymbol{\nabla})\boldsymbol{B} + (\boldsymbol{B} \cdot \boldsymbol{\nabla})\boldsymbol{v} - \boldsymbol{B}\,(\boldsymbol{\nabla} \cdot \boldsymbol{v}) \; . \tag{25}$$

While the first term on the right-hand side describes the advection of magnetic field, the last two terms describe the amplification by shear (second term) and compression (third term).

Table 1 shows values for η, L, U R_m, P_m and τ_d for different astrophysical objects and laboratory experiments. Here $P_\mathrm{m} = \nu/\eta$ denotes the magnetic

Table 1: Characteristic values for the magnetic Reynolds number R_m and diffusion time scales for the core of the Earth, the Sun and laboratory liquid sodium experiments

Object	$\eta[\mathrm{m}^2/\mathrm{s}]$	$L[\mathrm{m}]$	$U[\mathrm{m/s}]$	R_m	P_m	τ_d
Earth (outer core)	2	10^6	10^{-3}	300	10^{-5}	10^4 years
Sun (molecular)	1	10^8	100	10^{10}	10^{-4}	10^9 years
Sun (turbulent)	10^8	10^8	100	100	~ 1	3 years
lab experiment	0.1	1	10	100	10^{-5}	10 s

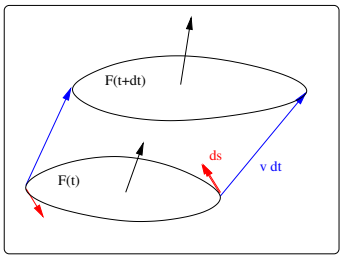

Figure 1: The closed line ∂F is moving with the fluid ('frozen into the fluid'). The area elements $-\int_{F(t)} d\boldsymbol{f}$, $\int_{\partial F} d\boldsymbol{s} \times \boldsymbol{v}\Delta t$ and $\int_{F(t+\Delta t)} d\boldsymbol{f}$ form a closed surface.

Prandtl number (ratio of viscosity and magnetic diffusivity). For the Sun we have given two values, assuming the molecular diffusivity and the turbulent diffusivity, which we introduce in more detail later. The values we show reflect the conditions close to the base of the convection zone; the Reynolds and Prandtl numbers for the photosphere are about 10^5 and 10^{-7}, respectively. Based on the molecular diffusivity the diffusion time scale is of the same order as the age of the Sun. This number however only applies to the radiative zone of the Sun (innermost 70% in radius), where the stratification is stable (no convection). It is conceivable that a magnetic field has endured in the core of the Sun without additional support from induction effects (primordial magnetic field) if a magnetic field was present in the interstellar cloud from which the Sun formed.

2.3.1 Alfvén's theorem: frozen-in flux

Let Φ be the magnetic flux through a surface F with the property that its boundary ∂F is moving with the fluid:

$$\Phi = \int_F \boldsymbol{B} \cdot d\boldsymbol{f} \; . \tag{26}$$

The total time derivative of Φ can be written as

$$\frac{d\Phi}{dt} = \lim_{\Delta t \to 0} \frac{1}{\Delta t} \left\{ \int_{F(t+\Delta t)} \boldsymbol{B}(t+\Delta t) \cdot d\boldsymbol{f} - \int_{F(t)} \boldsymbol{B}(t) \cdot d\boldsymbol{f} \right\} \tag{27}$$

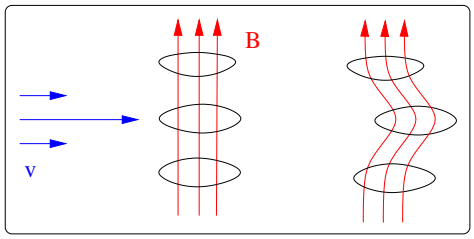

Figure 2: Shearing of a flux tube by a velocity field in ideal MHD

$$
\begin{aligned}
&= \lim_{\Delta t\to 0}\frac{1}{\Delta t}\left\{\int_{F(t+\Delta t)}[\boldsymbol{B}(t+\Delta t)-\boldsymbol{B}(t)]\cdot d\boldsymbol{f}\right.\\
&\quad\left.+\int_{F(t+\Delta t)}\boldsymbol{B}(t)\cdot d\boldsymbol{f}-\int_{F(t)}\boldsymbol{B}(t)\cdot d\boldsymbol{f}\right\}\\
&= \int_F\frac{\partial\boldsymbol{B}}{\partial t}\cdot d\boldsymbol{f}-\int_{\partial F}(\boldsymbol{v}\times\boldsymbol{B})d\boldsymbol{s}\\
&= \int_F\left[\frac{\partial\boldsymbol{B}}{\partial t}-\boldsymbol{\nabla}\times(\boldsymbol{v}\times\boldsymbol{B})\right]d\boldsymbol{f}=0\,.
\end{aligned}
$$

Here we used that the area elements $-\int_{F(t)}d\boldsymbol{f}$, $\int_{\partial F}d\boldsymbol{s}\times\boldsymbol{v}\Delta t$ and $\int_{F(t+\Delta t)}d\boldsymbol{f}$ form in the limit $\Delta t\to 0$ a closed surface (see Fig. 1), so that $\boldsymbol{\nabla}\cdot\boldsymbol{B}=0$ leads to

$$
\int_{F(t+\Delta t)}\boldsymbol{B}\cdot d\boldsymbol{f}-\int_{F(t)}\boldsymbol{B}\cdot d\boldsymbol{f}+\Delta t\int_{\partial F}\boldsymbol{B}\,(d\boldsymbol{s}\times\boldsymbol{v})=0\,. \tag{28}
$$

Thus the magnetic flux through a surface F with a boundary ∂F that is co-moving with the fluid is conserved. The effect of a shear flow on a magnetic flux tube (bundle of field lines) is illustrated in Fig. 2. In the limit of ideal MHD magnetic field lines are 'frozen into the fluid', which is a useful way to illustrate induction effects. In general it does not make sense to talk about moving magnetic field lines, since a field line is a mathematical construct with no physical identity. Since in the case of ideal MHD a field line is also a material line moving with the plasma, the concept of a 'moving' field line can be useful, but has to be used with care.

3 Dynamo problem

3.1 Motivation

We discussed in Sect. 2.3 that in the absence of induction effects magnetic fields decay on a time scale $\tau_d\sim L^2/\eta$ (Eq. [23]). An indication of dynamo action is the presence of magnetic field on a time scale $t\gg\tau_d$.

In the case of the Earth, studies of rock magnetism show that a magnetic field (in strength comparable to the current field) has been present over geological

time scales of the order of 3.5×10^9 years, which is significantly longer than the diffusion time $\tau_d \sim 10^4$ years. The magnetic field of the Earth must be maintained by dynamo action (any other type of permanent rock magnetism is ruled out because the temperature in the core is above the Curie point).

In the case of the Sun, magnetic activity can be traced back through ice core measurements of cosmogenic isotopes such as ^{10}Be. For the past 3×10^5 years these measurements show a persistent 11 year cycle disrupted by epochs of reduced solar activity spanning of the order of 100 to 200 years. Also stellar observations indicate that solar-like magnetic activity is common among stars with outer convection zones. On the other hand we showed in table 1 that the molecular diffusion time of about $\sim 10^9$ years is (within one order of magnitude) comparable to the typical life time of a solar-like star. Unlike in the case of the geodynamo this is not enough evidence for dynamo action and alternative explanations for the solar magnetism have been proposed based on the idea of a torsional oscillator periodically amplifying a primordial poloidal field frozen into the core of the Sun. However, this would require significant changes of the internal rotation of the Sun, changing the sign of the rotational shear in a way that is not consistent with the almost steady differential rotation observed by helioseismology. As shown in Table 1, turbulent motions in the convection zone of the Sun (outermost 30%) significantly reduce the effective diffusion time scale so that also here dynamo action is required to explain the observed activity.

3.2 A brief history of dynamo theory

Larmor (1919) was the first who asked how a body like the Sun can become a magnet. At that time he suggested already the possibility that the motion of an electrically conducting fluid across magnetic field lines in a rotating body could create the currents required to maintain that field. In the following decades 'advances' in dynamo theory were mainly made through the discovery of anti-dynamo theorems that rule out simple field and flow structures, which makes the investigation of possible dynamos rather complicated and hindered theoretical progress for a few decades. The most famous anti-dynamo theorem on the impossibility of axisymmetric dynamo action was found by Cowling (1933) and many generalizations and additional theorems followed. The search for a general anti-dynamo proof was brought to an end with the examples of Herzenberg (1958) and Backus (1958) that rigorously demonstrated that dynamo action as defined in Sect. 3.3 is possible. While these examples consisted of laminar flows (uniformly rotating spheres embedded into a conducting fluid) the first big breakthrough for astrophysical (turbulent) dynamos was made by Parker (1955), who realized that the dynamo problem can be simplified by averaging over the non-axisymmetric complicated parts and deriving an equation for an (axisymmetric) mean field. This approach was later mathematically refined by Braginskii (1964) and Steenbeck et al. (1966). Mean field theory allowed for fundamental theoretical study of dynamo theory and has been used since then as the main mathematical framework for many decades. For a summary of mean field theory we refer to Rüdiger & Hollerbach (2004). Among the more recent

developments is the addition of advection caused by the meridional circulation (see Sect. 3.7). With the advances in computing power, 3D numerical simulations of the full MHD equations (with some approximations) have become a powerful tool for studying dynamos over the last 2 decades. In the following sections we focus primarily on mean field theory to introduce the basic concepts of large-scale turbulent dynamo theory. In the end we discuss the limitations of mean field theory and summarize some results from 3D numerical simulations. For further reading we also recommend the textbooks on dynamo theory by Moffatt (1978) and Proctor & Gilbert (1995) and the review of non-linear dynamo theory by Brandenburg & Subramanian (2005).

3.3 Definition of dynamo problem

Let S be a volume filled with conducting fluid, bounded by a surface ∂S. We are looking for a smooth solution $\boldsymbol{B}$ that is produced by currents contained within S, decays asymptotically as r^{-3} for $r \to \infty$, is solenoidal ($\boldsymbol{\nabla} \cdot \boldsymbol{B} = 0$) and is a solution of the system

$$\begin{aligned} \frac{\partial \boldsymbol{B}}{\partial t} &= \boldsymbol{\nabla} \times (\boldsymbol{v} \times \boldsymbol{B} - \eta \, \boldsymbol{\nabla} \times \boldsymbol{B}) \qquad \text{in } S \\ \boldsymbol{\nabla} \times \boldsymbol{B} &= 0 \qquad\qquad\qquad\qquad\quad \text{outside } S \\ [\boldsymbol{B}] &= 0 \;\; \text{(B continuous)} \qquad \text{across } \partial S \end{aligned} \tag{29}$$

We further assume that the smooth velocity field $\boldsymbol{v}$ vanishes outside S and is tangent to the boundary ($\boldsymbol{n} \cdot \boldsymbol{v} = 0$ on ∂S), and that the kinetic energy within S has an upper bound:

$$E_{\rm kin} = \int_S \frac{1}{2} \varrho \boldsymbol{v}^2 \, dV \le E_{\rm max} \quad \forall \, t \, . \tag{30}$$

The velocity field $\boldsymbol{v}$ acts as a dynamo if an initial condition $\boldsymbol{B} = \boldsymbol{B}_0$ exists for which the magnetic energy

$$E_{\rm mag} = \int_{-\infty}^{\infty} \frac{1}{2\mu_0} \boldsymbol{B}^2 \, dV \tag{31}$$

does not approach zero as $t \to \infty$.

The formal difference between the type of dynamos that we are interested in here and the self-excited dynamos in power plants is the homogeneous distribution of conductivity (that would lead to a short-circuit situation) that does not put any constraints on electric currents (electric wires could be considered as special case of a highly inhomogeneous conductivity distribution). For this reason these dynamos are also called homogeneous fluid dynamos.

3.4 Basic ingredients of a dynamo

Fig. 3 illustrates the basic ingredients required to amplify a closed magnetic field loop. After a full cycle, the magnetic field strength and the flux have doubled (two loops, each with the original magnetic flux) and the process can be

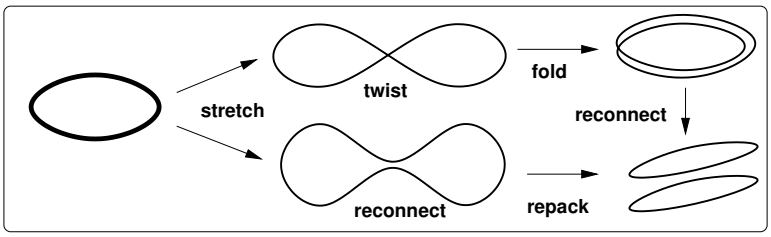

Figure 3: Illustration of 2 possible flux-rope dynamos. In both cases the field amplification takes place during the stretch operation. The twist-fold (top) and reconnect-repack (bottom) steps are required to remap the amplified flux-rope into the original volume element so that the process can be repeated. Magnetic diffusivity is essential to allow for the topology change required to close the cycle. Each cycle increases the field strength by a factor of 2.

repeated. This very simple illustration points out already a few fundamental properties of a dynamo process. In order to be able to remap the magnetic field configuration into the original volume element, three-dimensional motions are required. Amplification through stretching is possible in a strictly two-dimensional domain, but there is no way to move the resulting field to return to the right-hand side of the image. The two examples also point out the crucial role of diffusivity in changing the topology of the field. The 'stretch-twist-fold' mechanism (excluding diffusive steps) leads to loops of increased complexity, while the 'stretch-reconnect-repack' process explicitly involves magnetic diffusivity and ends up with two flux ropes of similar topology. A reconnection step at the end of the 'stretch-twist-fold' process leads a similar result. In the case of the 'stretch-twist-fold' dynamo the sign of the twist does not matter. Note that neither mechanism requires a flow with a net kinetic helicity.

3.5 Large-scale and small-scale dynamos

The definition of the dynamo problem we give in Sect. 3.3 only focuses on the asymptotic behavior of the magnetic energy and does not imply anything about the structure of the magnetic field. Most astrophysical objects have turbulent velocity fields with a correlation length scale l_c that is much smaller than the scale of the star or planet. Nevertheless these objects have a magnetic field that has a length scale much larger than l_c and also evolves over time scales much larger than the correlation times scale of the turbulence. If we decompose the magnetic field into a large-scale part and a small-scale part by writing $\boldsymbol{B} = \overline{\boldsymbol{B}} + \boldsymbol{B}'$, we can express the magnetic energy as

$$E_{\rm mag} = \int \frac{1}{2\mu_0} \overline{\boldsymbol{B}}^2 \, dV + \int \frac{1}{2\mu_0} \overline{\boldsymbol{B}'^2} \, dV \; . \tag{32}$$

We call a dynamo a small-scale dynamo if the magnetic energy is mainly in the small scales (energy carrying scales of the turbulence), meaning $\overline{\boldsymbol{B}}^2 \ll \overline{\boldsymbol{B}'^2}$. On

the other hand, a large-scale dynamo produces a magnetic field with a scale comparable to the planet or star. In this case we have at least $\overline{\boldsymbol{B}}^2 \sim \overline{\boldsymbol{B}'^2}$. While almost any chaotic (turbulent) velocity field is a small scale dynamo for a sufficiently large R_m, a large-scale dynamo requires an inverse cascade that produces magnetic energy on a scale larger than the energy carrying scale of the turbulence. This requires certain large-scale properties in the flow field such as mean helicity and shear as we discuss later. There is no sharp distinction between small and large-scale dynamos and both can be present at the same time.

Three-dimensional numerical MHD simulations ((Cattaneo 1999), (Vögler & Schüssler 2007)) have shown that almost all turbulent velocity fields lead to small-scale dynamo action, provided the magnetic Reynolds number is large enough. For numerical reasons most small-scale dynamo simulations were done in a setup in which the viscosity ν and the magnetic diffusivity η were similar, while in stellar convection zones typically $\nu \ll \eta$. It is a current research topic to which extent small-scale dynamos are affected by the magnetic Prandtl number $P_\mathrm{m} = \nu/\eta$. A small value of P_m implies that the dissipative scale of the velocity field is much smaller than the dissipative scale of the magnetic field. This means that on the smallest scale of the magnetic field the velocity field is still turbulent and therefore more dissipative; in the case of a large value of P_m the velocity field is smooth even on the smallest scales of the field, and therefore more effective in amplifying field on that scale.

3.6 Slow and fast dynamos

We pointed out in Sect. 3.4 the important role of magnetic diffusivity in the dynamo process as it allows changes of field topology. A further distinction of dynamos is made with respect to the dependence of the growth rate of magnetic field on the magnetic Reynolds number (Eq. [21]). If the growth rate of a dynamo is given by a kinematic time scale L/v_rms that is asymptotically independent of R_m as $R_\mathrm{m} \to \infty$ it is called a fast dynamo, while a dynamo is called a slow dynamo if the growth rate is explicitly influenced by the microscopic diffusivity and vanishes as $R_\mathrm{m} \to \infty$. The distinction between fast and slow dynamos is only relevant in the initial kinematic growth phase of the magnetic field in which the feedback of the Lorenz force on the flow field is not important (see Eq. [2]). Fast dynamo action is only possible, if the length-scale l at which reconnection takes place decreases at least as $R_\mathrm{m}^{-1/2}$ with increasing R_m so that $\tau_d \sim l^2/\eta \sim L^2/(R_\mathrm{m}\eta) \sim L/v_\mathrm{rms}$. Fast dynamos are of particular interest for astrophysical systems since the magnetic Reynolds number is typically very large (e.g., 10^9 for the Sun).

For a comparative review of large and small-scale dynamos in the solar convection zone as well as the fast dynamo problem we refer to Cattaneo & Hughes (2001).

3.7 Effect of differential rotation and meridional flow

Most spherical large-scale dynamos (planets and Sun) show an almost dipolar axisymmetric field. We analyze here the most simple situation: The effect of an axisymmetric flow on an axisymmetric magnetic field. The two components of an axisymmetric flow are differential rotation (flow in longitudinal, or ϕ-direction) and meridional circulation (flow in radial and latitudinal direction, $r-\theta$-plane). While these flows are not very important in the case of the outer core of the Earth, all stars with outer convection zones show strong differential rotation, which is expected to have a significant role in stellar dynamos. A meridional circulation is coupled to differential rotation through the Coriolis force and has been identified by Choudhuri et al. (1995) and Dikpati & Charbonneau (1999) as major ingredient in the case of the solar dynamo.

Any axisymmetric, solenoidal ($\boldsymbol{\nabla} \cdot \boldsymbol{B} = 0$) field can be written in spherical coordinates as

$$\boldsymbol{B} = B\boldsymbol{e_\Phi} + \boldsymbol{\nabla} \times (A\boldsymbol{e_\Phi}) \,, \tag{33}$$

where B is the toroidal field and the contour-lines of $A\, r \sin\theta$ are the field lines of the poloidal field. Together with the velocity field

$$\boldsymbol{v} = v_r\boldsymbol{e_r} + v_\theta\boldsymbol{e_\theta} + \Omega\, r \sin\theta \boldsymbol{e_\Phi} \tag{34}$$

this leads to the induction equation in spherical coordinates

$$\begin{aligned} \frac{\partial B}{\partial t} \quad + \quad & \frac{1}{r}\left(\frac{\partial}{\partial r}(r v_r B) + \frac{\partial}{\partial \theta}(v_\theta B)\right) = \\ & r \sin \boldsymbol{B}_p \cdot \boldsymbol{\nabla}\Omega + \eta\left(\Delta - \frac{1}{(r\sin\theta)^2}\right) B \end{aligned} \tag{35}$$

$$\frac{\partial A}{\partial t} \quad + \quad \frac{1}{r\sin\theta}\, \boldsymbol{v}_p \cdot \boldsymbol{\nabla}(r\sin\theta A) = \eta\left(\Delta - \frac{1}{(r\sin\theta)^2}\right) A \,, \tag{36}$$

where Δ denotes the Laplace operator, $\boldsymbol{B}_p = (B_r, B_\theta, 0)$ the poloidal component of the magnetic field and $\boldsymbol{v}_p = (v_r, v_\theta, 0)$ the meridional flow (poloidal component of the velocity). Here we further assumed that η is uniform and constant.

The time evolution of the poloidal field is decoupled from the toroidal field and the poloidal component of the field has only decaying solutions: $A \to 0$ for $t \to \infty$. The time evolution of the toroidal field is coupled to the poloidal field through the Ω-effect (or more exactly $\boldsymbol{\nabla}\Omega$-effect), which can act as source term preventing decay of the toroidal field. Since $\boldsymbol{B}_p \to 0$ for $t \to \infty$ this source term decays and we have also $B \to 0$ for $t \to \infty$.

This discussion shows that an axisymmetric magnetic field cannot be maintained by an axisymmetric flow. We show in Sect. 3.8 that this statement remains valid also for non-axisymmetric flows. On the other hand if we allow for non-axisymmetric magnetic field, axisymmetric flows can act as dynamo (see e.g. the dynamo proposed by Gailitis (1970)). However, purely toroidal motions in spherical geometry cannot be a dynamo if $\eta = \eta(r)$ (toroidal theorem: (Elsasser 1946), (Bullard & Gellman 1954) and (Backus 1958)).

3.8 Cowling's anti-dynamo theorem

Given the fact that in the solar convection zone the magnetic Reynolds number is of the order of $10^5 - 10^9$ one would expect that it is easy for fluid motions to overcome the resistive dissipation and that it should be easy to identify a velocity field with a dynamo property. The difficulty arises from topological constraints on the magnetic field and the velocity field. Cowling's anti-dynamo theorem rules out the most simple geometries for dynamo generated magnetic fields:

No axisymmetric magnetic field with currents limited to a finite volume in space can be maintained by a flow with finite amplitude.

The original theorem of Cowling (1933) assumed a stationary magnetic field and we present the basic idea of the proof for a poloidal field below. In the meantime the theorem has been proven in more general situations allowing also for time-dependent solutions.

In the case of a stationary magnetic field we have $\boldsymbol{\nabla} \times \boldsymbol{E} = -\partial \boldsymbol{B}/\partial t = 0$ and can express the electric field through a potential Ψ. In that case Ohm's law is given by $\boldsymbol{j} = \sigma(\boldsymbol{v} \times \boldsymbol{B} - \boldsymbol{\nabla}\Psi)$. Having an axisymmetric field requires that the poloidal field $\boldsymbol{B}_p$ has at least one O-type neutral line (in the toroidal direction) on which the poloidal field strength vanishes. On the other hand the toroidal electric current along this line $\mu_0 \boldsymbol{j}_t = \boldsymbol{\nabla} \times \boldsymbol{B}_p$ does not vanish and has to be maintained by the toroidal component of $\boldsymbol{v} \times \boldsymbol{B} - \boldsymbol{\nabla}\Psi$. The electric field does not contribute since axisymmetry requires $\partial\Psi/\partial\phi = 0$ and $(\boldsymbol{v} \times \boldsymbol{B})_t = (\boldsymbol{v}_p \times \boldsymbol{B}_p)$ vanishes since B_p vanishes at the neutral line. Therefore an axisymmetric poloidal field cannot be maintained by a flow. This proof can be generalized to the case of a neutral point of higher order in which both B_p and its derivatives vanish. We refer here to text books (e.g., Moffatt (1978)) for an in-depth discussion.

4 Mean-field theory

In this section, we focus on the processes capable of maintaining a large-scale magnetic field. To this end we decompose the magnetic field into a large-scale 'mean' field and the small-scale components through an averaging procedure. We assume in the following that the averaging procedure obeys the Reynolds rules: For any function f and g decomposed as $f = \overline{f} + f'$ and $g = \overline{g} + g'$, were the bar indicates the averaged and the prime the fluctuating quantity, we require that

$$\overline{\overline{f}} = \overline{f} \longrightarrow \overline{f'} = 0 \tag{37}$$

$$\overline{f+g} = \overline{f} + \overline{g} \tag{38}$$

$$\overline{f\overline{g}} = \overline{f}\,\overline{g} \longrightarrow \overline{f'\overline{g}} = 0 \tag{39}$$

$$\overline{\partial f/\partial x_i} = \partial \overline{f}/\partial x_i \tag{40}$$

$$\overline{\partial f/\partial t} = \partial \overline{f}/\partial t\,. \tag{41}$$

The averaging procedures that are of interest in the context of mean-field theory are the ensemble average (meaning a chaotic system is averaged over several representations of the chaotic system) and the longitudinal average, in which $\overline{\boldsymbol{B}}$ reflects the axisymmetric component of the large-scale magnetic field (multipole series with $m = 0$).

4.1 Mean-field induction equation

We follow here a derivation of the mean-field electrodynamics following closely Rädler (1980) and Rädler & Stepanov (2006). In order to derive an equation for the time evolution of the mean field we apply the averaging procedure to the induction equation Eq. (4) which leads to

$$\frac{\partial \overline{\boldsymbol{B}}}{\partial t} = \boldsymbol{\nabla} \times \left(\overline{\boldsymbol{v}' \times \boldsymbol{B}'} + \overline{\boldsymbol{v}} \times \overline{\boldsymbol{B}} - \eta \boldsymbol{\nabla} \times \overline{\boldsymbol{B}} \right) . \tag{42}$$

The new term which enters this equation compared to the original induction equation is the second order correlation electromotive force (EMF)

$$\overline{\boldsymbol{\mathcal{E}}} \equiv \overline{\boldsymbol{v}' \times \boldsymbol{B}'} . \tag{43}$$

While the fluctuating velocity component $\boldsymbol{v}'$ is assumed to be known (kinematic approach), $\boldsymbol{B}'$ has to be computed from the induction equation. An equation for $\boldsymbol{B}'$ can be derived by subtracting the mean-field induction equation Eq. (42) from the microscopic induction equation Eq. (4), which leads to

$$\frac{\partial \boldsymbol{B}'}{\partial t} = \boldsymbol{\nabla} \times \left(\boldsymbol{v}' \times \overline{\boldsymbol{B}} + \overline{\boldsymbol{v}} \times \boldsymbol{B}' - \eta \boldsymbol{\nabla} \times \boldsymbol{B}' + \boldsymbol{v}' \times \boldsymbol{B}' - \overline{\boldsymbol{v}' \times \boldsymbol{B}'} \right) . \tag{44}$$

It is in general only possible to solve this equation by making strong assumptions, primarily because of the terms that are quadratic in the fluctuating quantities (closure problem). We return to this path in Sect. 4.3 and discuss the mean-field induction equation first based on more general symmetry properties which do not require an explicit solution for $\boldsymbol{B}'$.

4.2 Symmetry constraints on turbulent induction effects

For a given velocity field $\boldsymbol{v}$ (kinematic approach) it follows from the induction equation for the fluctuating field Eq. (44) that $\boldsymbol{B}'$ is a linear functional of $\overline{\boldsymbol{B}}$, so that also the electromotive force $\overline{\boldsymbol{\mathcal{E}}}$ (Eq. [43]) has to be a linear functional of $\overline{\boldsymbol{B}}$. In general $\boldsymbol{B}'$ does not have to vanish if $\overline{\boldsymbol{B}}$ does, since the velocity field $\boldsymbol{v}'$ could also support a small scale dynamo. For simplicity we assume in the following that $\boldsymbol{B}'$ vanishes if $\overline{\boldsymbol{B}}$ does, assuming that any $\boldsymbol{B}'$ produced by a small scale dynamo correlates only weakly with $\boldsymbol{v}'$ (if the latter is not the case, the following equations would have to be modified by adding an inhomogeneous source term not dependent on $\overline{\boldsymbol{B}}$). We can therefore express the components $\overline{\mathcal{E}}_i$ as

$$\overline{\mathcal{E}}_i(\boldsymbol{x}, t) = \int_{-\infty}^{\infty} d^3x' \int_{-\infty}^{t} dt' \, \mathcal{K}_{ij}(\boldsymbol{x}, t, \boldsymbol{x}', t') \, \overline{B}_j(\boldsymbol{x}', t') . \tag{45}$$

The kernel $\mathcal{K}$ is dependent on average quantities of the fluctuating velocity field $\boldsymbol{v}'$ as well as the mean flow $\overline{\boldsymbol{v}}$. Assuming that the turbulence has finite correlation length and time scales l_c and τ_c, significant contributions in Eq. (45) only arise for $|\boldsymbol{x}-\boldsymbol{x}'|<l_c$ and $t-t'<\tau_c$. In order to derive more simplified (interpretable) expressions we now introduce the concept of a scale separation by assuming that the length and times scales of the mean field are much larger than l_c and τ_c. Unfortunately, this assumption is for most astrophysical applications only marginally justified. Turbulence has a continuous spectrum ranging from a large energy carrying scale down to the dissipative scale. The scale of the largest eddies is often not too different from the largest scales of the system, e.g., in the case of the solar convection zone the large scale of the turbulence spectrum is of the order of a pressure scale height at the base of the convection zone, which is about a third of the convection zone depth. We refer to Sect. 5.1 for a more detailed discussion of the limitations of the mean-field approach.

Under the assumption of a sufficient scale separation we take care of the non-locality in space by using a Taylor-expansion of $\overline{\mathbf{B}}$. For simplification we drop any non-locality in time here (see Sect. 5.1 for more discussion on that). This leads to the expansion

$$\overline{\mathcal{E}}_i = a_{ij}\overline{B}_j + b_{ijk}\frac{\partial \overline{B}_j}{\partial x_k} + \ldots \tag{46}$$

From the induction equation of the form of Eq. (25) we see that the terms $\sim b_{ijk}$ result from the advection term, while the field line stretching and compression terms lead to expressions $\sim a_{ij}$. We rewrite this expression by decomposing the tensors into symmetric and antisymmetric parts

$$\begin{aligned} a_{ij} &= \underbrace{\frac{1}{2}\left(a_{ij}+a_{ji}\right)}_{\alpha_{ij}} + \underbrace{\frac{1}{2}\left(a_{ij}-a_{ji}\right)}_{-\frac{1}{2}\varepsilon_{ijk}\gamma_k} \\ \frac{\partial \overline{B}_j}{\partial x_k} &= \frac{1}{2}\left(\frac{\partial \overline{B}_j}{\partial x_k}+\frac{\partial \overline{B}_k}{\partial x_j}\right) + \underbrace{\frac{1}{2}\left(\frac{\partial \overline{B}_j}{\partial x_k}-\frac{\partial \overline{B}_k}{\partial x_j}\right)}_{-\frac{1}{2}\varepsilon_{jkl}(\boldsymbol{\nabla}\times\overline{\boldsymbol{B}})_l} . \end{aligned} \tag{47}$$

Here, we indicated that the antisymmetric tensors can be expressed through a vector and the Levi-Civita tensor ε_{ijk}. This leads to the mathematically equivalent tensor equation with the turbulent transport coefficients $\boldsymbol{\alpha}$, $\boldsymbol{\beta}$, $\boldsymbol{\gamma}$ and $\boldsymbol{\delta}$

$$\overline{\boldsymbol{\mathcal{E}}} = \boldsymbol{\alpha}\overline{\boldsymbol{B}} + \boldsymbol{\gamma}\times\overline{\boldsymbol{B}} - \boldsymbol{\beta}\,\boldsymbol{\nabla}\times\overline{\boldsymbol{B}} - \boldsymbol{\delta}\times(\boldsymbol{\nabla}\times\overline{\boldsymbol{B}}) + \ldots \tag{48}$$

Here, we also split the tensor in front of $\boldsymbol{\nabla}\times\overline{\boldsymbol{B}}$ in a symmetric part $\boldsymbol{\beta}$ and introduce a vector $\boldsymbol{\delta}$ for the antisymmetric part. In the mean-field expansion Eq. (48) we left out the term proportional to the symmetric part of $\partial\overline{B}_j/\partial x_k$ since it does not lead to physical effects that are distinct from what is already contained in $\boldsymbol{\alpha}$, $\boldsymbol{\beta}$, $\boldsymbol{\gamma}$ and $\boldsymbol{\delta}$. The relation to the original expression a_{ij} and b_{ijk}

is given by

$$\alpha_{ij} = \frac{1}{2}\left(a_{ij}+a_{ji}\right) , \qquad \gamma_i = -\frac{1}{2}\varepsilon_{ijk}a_{jk}$$
$$\beta_{ij} = \frac{1}{4}\left(\varepsilon_{ikl}b_{jkl}+\varepsilon_{jkl}b_{ikl}\right) , \qquad \delta_i = \frac{1}{4}\left(b_{jji}-b_{jij}\right) . \tag{49}$$

From the mathematical form of Eq. (48) we can see already that the γ-effect acts like an advection and that the β- and δ-terms can be interpreted as an anisotropic magnetic diffusivity. The α-effect is a completely new effect and the most important one for large-scale dynamo action. We discuss the physical meaning of these terms in more detail in Sect. 4.3.

The vectors and tensors $\boldsymbol{\alpha}$, $\boldsymbol{\beta}$, $\boldsymbol{\gamma}$ and $\boldsymbol{\delta}$ are large-scale correlations of the small-scale velocity field $\boldsymbol{v}'$. They have to reflect the same large-scale symmetries as the MHD equations $\boldsymbol{v}'$ is derived from. In the absence of any preferred direction they have to be homogeneous and isotropic, which means that the only possible construction elements are the isotropic homogeneous tensors δ_{ij} and ε_{ijk}. If the system has an additional preferred direction, such as gravity or rotation, also g_i and Ω_i are directional quantities entering $\boldsymbol{\alpha}$, $\boldsymbol{\beta}$, $\boldsymbol{\gamma}$ and $\boldsymbol{\delta}$. In that case additional tensors can be formed from vector quantities through the dyadic product leading to expressions such as $a_{ij} = g_i\Omega_j$.

An additional property of the mean-field expansion Eq. (48) is that it relates the axial (pseudo) vector $\boldsymbol{B}$ to the polar (true) vector $\boldsymbol{E}$. Polar and axial vectors transform similarly under transformations that do not change the handedness of a coordinate system but transform differently under an improper rotation (inversion + proper rotation). A coordinate inversion $\boldsymbol{x} \to -\boldsymbol{x}$ is an example of an improper rotation in 3D (but not in 2D). Let us consider two polar vectors $\boldsymbol{a}$ and $\boldsymbol{b}$ and an axial vector $\boldsymbol{c} = \boldsymbol{a} \times \boldsymbol{b}$. The inversion leads to $\boldsymbol{a} \to -\boldsymbol{a}$, $\boldsymbol{b} \to -\boldsymbol{b}$, but $\boldsymbol{c} \to \boldsymbol{c}$. Note that the inversion of the vector components with respect to the basis implies that a polar vector remains unchanged (the basis is pointing in the opposite direction, too), while an axial vector actually changes direction. Physical examples of axial (pseudo) vectors other than the magnetic field include angular momentum, torque, vorticity and angular velocity. The concept of pseudo vectors can also be expanded to tensors of any rank. The most famous pseudo tensor of third rank is the Levi-Civita tensor ε_{ijk} and most examples of pseudo vectors mentioned above are related to polar vectors by ε_{ijk} (cross product and curl). Additional pseudo tensors that are important here are those formed through the dyadic product, e.g. expressions such as $g_i\Omega_j$, which is a pseudo tensor of second rank since $\boldsymbol{g}$ is a polar and $\boldsymbol{\Omega}$ is an axial vector. On the other hand an expression such as $\Omega_i\Omega_j$ is again a true tensor.

All pseudo vectors have in common that their definition depends on the handedness of the coordinate system, which is pure convention (except for the weak force where the chirality of the universe matters). The difference between vectors and pseudo vectors becomes important if one wants to exploit the symmetries of a physical system. Since electromagnetism does not have an intrinsic handedness, the mean-field expansion Eq. (48) has to be invariant under inversions (changing right handed to left handed coordinate systems). Therefore $\boldsymbol{\delta}$

and $\boldsymbol{\alpha}$ have to be pseudo tensors, while $\boldsymbol{\gamma}$ and $\boldsymbol{\beta}$ are true tensors. This sets constraints on the combinations of the pseudo tensors Ω_i and ε_{ijk} and the true tensors g_i and δ_{ij} that are allowed to construct $\boldsymbol{\alpha}$, $\boldsymbol{\beta}$, $\boldsymbol{\gamma}$ and $\boldsymbol{\delta}$.

Considering only terms that are not more than second order in g and Ω we have the following expressions for the turbulent induction effects:

$$\begin{aligned} \alpha_{ij} &= \alpha_0(\boldsymbol{g}\cdot\boldsymbol{\Omega})\delta_{ij} + \alpha_1\left(g_i\Omega_j + g_j\Omega_i\right) , \quad & \gamma_i &= \gamma_0 g_i + \gamma_1\varepsilon_{ijk}g_j\Omega_k \\ \beta_{ij} &= \beta_0\,\delta_{ij} + \beta_1\,g_ig_j + \beta_2\,\Omega_i\Omega_j , & \delta_i &= \delta_0\Omega_i . \end{aligned} \tag{50}$$

The scalar coefficients $\alpha_0, \ldots, \delta_0$ are typically functions of the rms-velocity and correlation time scale of the turbulence field. Since they can be also zero, the following discussion can give only necessary conditions for the existence of the various turbulent induction effects.

In the case of isotropic homogeneous turbulence only a term $\beta_{ij} = \beta_0\,\delta_{ij}$ can exist, which is interpreted as the isotropic turbulent diffusivity . For most astrophysical systems we have $\beta_0 \gg \eta$ as consequence of the large magnetic Reynolds number. In the presence of stratification ($\boldsymbol{g}$), horizontal and vertical diffusivities can differ, while rotation $\boldsymbol{\Omega}$ can introduce anisotropy with respect to the axis of rotation. The δ-effect, which contains the antisymmetric part of the diffusivity tensor, can exist in the case of rotation.

The advection-like γ-effect can exist in the case of stratification (transport in radius) or in higher order as consequence of stratification and rotation as longitudinal transport. The latter is of interest since it can mimic the effect of differential rotation. The most important contribution to the radial transport results in the case of stratification from anisotropies between upflow and downflows. Since upflows have to expand and downflows have to compress as consequence of stratification, downflows have typically a smaller filling factor and larger velocity amplitudes. The net effect of this anisotropy on the magnetic field is typically a downward directed transport also called turbulent pumping.

Unlike the other effects, the α-effect can only exist if stratification and rotation are present at the same time. The reason for this constraint and the physics behind the α-effect become more evident in the next section, where we relate the turbulent induction effects directly to properties of the turbulent velocity field.

4.3 Dynamo coefficients from second order correlation approximation (SOCA)

After the more general discussion of turbulent induction effects based on symmetry in Sect. 4.2 we return now to the path left at the end of Sect. 4.1 and explicitly solve Eq. (44) for the fluctuating field, which requires in general significant simplifications. To illustrate this path we neglect the mean flow $\overline{\boldsymbol{v}}$. The higher order moments are obviously the terms most difficult to treat and can be neglected if $B' \ll \overline{B}$. The induction equation for the fluctuating field reduces then to

$$\left(\frac{\partial}{\partial t} - \eta\Delta\right)\boldsymbol{B}' = \boldsymbol{\nabla}\times\left(\boldsymbol{v}'\times\overline{\boldsymbol{B}}\right) . \tag{51}$$

The condition $B' \ll \overline{B}$ is fulfilled if either $R_\mathrm{m} \ll 1$ or the Strouhal number $S = \tau_c v/l_c \ll 1$. Unfortunately, neither of these conditions is fulfilled in stellar convection zones. We have $R_\mathrm{m} \gg 1$ and the second condition is only marginally fulfilled since $S \sim 1$; surprisingly this approach yields reasonable results nevertheless (which might indicate that contributions from the higher order terms correlate only weakly with $\boldsymbol{v}'$ and drop out when $\overline{\boldsymbol{\mathcal{E}}}$ is calculated). Integrating Eq. (51) leads in the limit of large R_m to

$$\boldsymbol{B}'(t) = \int_{-\infty}^{t} \boldsymbol{\nabla} \times [\boldsymbol{v}'(\tau) \times \overline{\boldsymbol{B}}(\tau)] d\tau \; . \tag{52}$$

The turbulent electromotive force is given by

$$\overline{\boldsymbol{\mathcal{E}}} = \int_{-\infty}^{t} \overline{\boldsymbol{v}'(t) \times [\boldsymbol{\nabla} \times (\boldsymbol{v}'(\tau) \times \overline{\boldsymbol{B}}(\tau)]} d\tau \; . \tag{53}$$

This expression for $\overline{\boldsymbol{\mathcal{E}}}$ accounts for non-locality in time and requires the computation of two-time correlations of the velocity field. For further simplification we reduce the correlations to single-time correlations by approximating

$$\int_{-\infty}^{t} \overline{v_i'(t) v_k'(\tau)} d\tau = \tau_c \overline{v_i'(t) v_k'(t)} \; . \tag{54}$$

Formally expressions containing the correlation between the velocity and a velocity gradient could have a different τ_c. For reasons of simplicity we use in the following a single τ_c for all expressions.

Expansion of these terms and rearrangement according to the mean-field expansion Eq. (48) leads to the following expressions

$$\begin{aligned} \alpha_{ij} &= \frac{1}{2}\tau_c \left(\varepsilon_{ikl} \overline{v_k' \frac{\partial v_l'}{\partial x_j}} + \varepsilon_{jkl} \overline{v_k' \frac{\partial v_l'}{\partial x_i}} \right) \; , \qquad \gamma_i = -\frac{1}{2}\tau_c \frac{\partial}{\partial x_k} \overline{v_i' v_k'} \\ \beta_{ij} &= \frac{1}{2}\tau_c \left(\overline{\boldsymbol{v}'^2} \delta_{ij} - \overline{v_i' v_j'} \right) \; , \qquad\qquad\qquad \delta_i = 0 \; . \end{aligned} \tag{55}$$

The fact that we do not get a δ-effect here is a consequence of the (optional) simplification we introduced through Eq. (54). Computing the trace of $\boldsymbol{\alpha}$ and $\boldsymbol{\beta}$ gives

$$\begin{aligned} \alpha_{ii} &= \tau_c \, \varepsilon_{ikl} \overline{v_k' \frac{\partial v_l'}{\partial x_i}} = -\tau_c \overline{v_k' \varepsilon_{kil} \frac{\partial v_l'}{\partial x_i}} = -\tau_c \overline{\boldsymbol{v}' \cdot (\boldsymbol{\nabla} \times \boldsymbol{v}')} \\ \beta_{ii} &= \tau_c \overline{\boldsymbol{v}'^2} \; . \end{aligned} \tag{56}$$

This shows that the magnitude of the turbulent magnetic diffusivity is directly related to the intensity of the turbulence. The α-effect, in contrast, is related to the kinetic helicity of the flow given by the expression

$$H_\mathrm{k} = \overline{\boldsymbol{v}' \cdot (\boldsymbol{\nabla} \times \boldsymbol{v}')} \; . \tag{57}$$

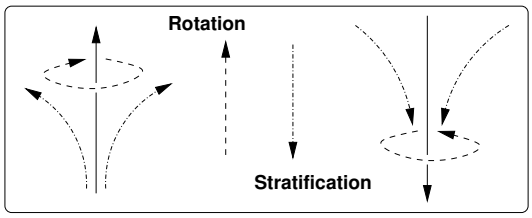

Figure 4: Mean helicity as consequence of stratification and rotation. The stratification leads to a correlation between the horizontal divergence and the vertical velocity. The influence of the Coriolis-force on the horizontal flows causes a mean kinetic helicity.

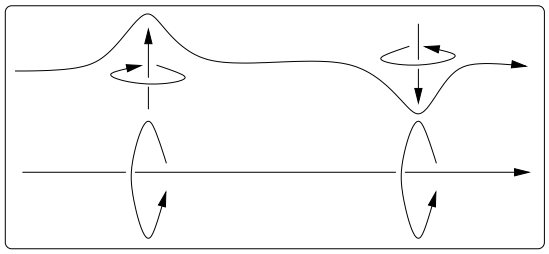

Figure 5: Relation between kinetic helicity and α-effect. The assumed negative kinetic helicity (left hand screw) induces a poloidal field with a current parallel to the toroidal field, leading to a positive α-effect. A net helicity is required to have up- and downward motions contributing the same way.

In a helical flow the velocity and vorticity are aligned with each other. Positive helicity corresponds to a right-handed screw, meaning that looking into the direction of the flow, fluid is moving clockwise. While in a turbulent flow H_k is in general locally different from zero, the α-effect requires that moreover the average of kinetic helicity does not vanish. A mean kinetic helicity is in general the consequence of stratification and rotation together as we show schematically in Figure 4. Rising convective motions lead to divergent horizontal flows (due to density stratification), which are turned into a left handed screw through the Coriolis force, leading to a negative flow helicity. Since downflows are accompanied by horizontal convergent flows, they also have a negative helicity, leading to a negative mean helicity of the flow. In Fig. 5 we illustrate the relation between kinetic helicity and α-effect for the case of negative kinetic helicity. A magnetic field originally contained within the plane shown (toroidal) is deformed and twisted leading to a component of field outside the plane (toroidal). A net helicity ensures that the contributions of up- and downwelling motions do not compensate each other and give a net contribution. Evaluating the expression for the α-effect Eq. (59) for the northern hemisphere of the solar convection zone, leads to a positive α-effect. A net correlation between vertical velocity and horizontal flow divergence only exists if the medium is stratified or close to

boundaries, which is in agreement with the finding of Sect. 4.2 that the α-effect requires an additional preferred direction beside rotation.

To further simplify the expressions derived from SOCA we can assume that the deviations from isotropy are small enough to neglect cross-correlations between different velocity components, but we still allow for inhomogeneity (variation of turbulence intensity with location), so that

$$\overline{{v_i}'{v_k}'} = \frac{1}{3}\overline{\boldsymbol{v}'^2}\delta_{ik} \; . \tag{58}$$

Under these assumptions the tensors $\boldsymbol{\alpha}$ and $\boldsymbol{\beta}$ become diagonal and can be expressed by scalar quantities

$$\alpha = \frac{1}{3}\alpha_{ii} = -\frac{1}{3}\tau_c \, \overline{\boldsymbol{v}' \cdot (\boldsymbol{\nabla} \times \boldsymbol{v}')} = \frac{1}{3} H_k \; , \qquad \eta_t = \frac{1}{3}\beta_{ii} = \frac{1}{3}\tau_c \, \overline{\boldsymbol{v}'^2} \; . \tag{59}$$

The γ-effect simplifies to

$$\boldsymbol{\gamma} = -\frac{1}{2}\boldsymbol{\nabla}\eta_t \; . \tag{60}$$

The assumptions required for these expressions are (1) validity of the kinematic approach (sufficiently weak field), (2) $B' \ll \overline{B}$ (either $R_\mathrm{m} \ll 1$ or $S = \tau_c v / l_c \ll 1$), (3) $\overline{\boldsymbol{v}} = 0$, (4) the introduction of τ_c by Eq. (54), and (5) isotropic, non-mirror symmetric turbulence (with weak inhomogeneity). While the assumptions (4) and (5) are not essential and were used primarily to simplify the expressions, the assumption (1) and (2) are crucial and at best marginally justified in most astrophysical applications. If (3) is not fulfilled the mean flow can lead to additional contributions if the advection time scale is comparable to the turbulent correlation time scale. The general form of Eq. (48) remains valid also when these conditions are not fulfilled; however, higher order terms might be relevant if scale separation is not well justified.

The expression Eq. (60) for the γ-effect is often also called turbulent diamagnetism, since it has the tendency to expel magnetic field from regions with increased turbulence intensity. In a stellar convection zone the turbulence intensity varies mainly in the radial direction, which leads to a radial transport. Toward the base of the convection zone the transport is downward directed since η_t drops there significantly (the amplitude of convective motions decreases since the fraction of energy flux transported through convection decreases smoothly to zero when approaching the base of the convection zone).

As we discussed above, the mean kinematic helicity required for the α-effect follows from a correlation between horizontal divergence and vertical motions as a result of stratification. A more detailed calculation for the turbulent α-effect leads to the result

$$\alpha \approx \alpha_0 (\boldsymbol{g} \cdot \boldsymbol{\Omega}) = \tau_c^2 v_\mathrm{rms}^2 \boldsymbol{\Omega} \cdot \boldsymbol{\nabla} \ln(\varrho v_\mathrm{rms}) \tag{61}$$

for the diagonal elements of the α tensor.

4.4 Energy equation for mean field

For the following discussion it will be helpful to derive an energy equation for the volume integrated energy of the mean field. Multiplication of the mean field induction equation Eq. (42) with $\overline{\boldsymbol{B}}$ and integration over the entire volume leads to

$$\frac{d}{dt}\int \frac{\overline{\boldsymbol{B}}^2}{2\mu_0}\,dV = -\mu_0 \int \eta \overline{\boldsymbol{j}}^2\,dV - \int \overline{\boldsymbol{v}}\cdot(\overline{\boldsymbol{j}}\times\overline{\boldsymbol{B}})\,dV + \int \overline{\boldsymbol{j}}\cdot\overline{\mathcal{E}}\,dV\ . \tag{62}$$

The first term on the right-hand side reflects resistive dissipation, the second term measures work done by mean flows against the mean Lorentz force (e.g. differential rotation), and the last term describes energy converted into the mean field by turbulent induction effects. The latter sustains the mean field if $\overline{\mathcal{E}}$ is on average pointing in the direction of the mean current.

4.5 Destruction of magnetic field: turbulent diffusivity

The derivation of the mean-field induction equation led to an additional dissipative term that significantly enhances the effective magnetic diffusivity in the presence of turbulence. In the case of isotropic, homogeneous turbulence the turbulent diffusivity is given by the scalar quantity (Eq. [59])

$$\eta_t = \frac{1}{3}\tau_c\,\overline{\boldsymbol{v}'^2} \sim L\,v_{\rm rms} \sim R_{\rm m}\eta \gg \eta\ . \tag{63}$$

Formally this term arises from the advection term in the induction equation Eq. (25), which is a non-dissipative transport term. The only dissipative term in the microscopic induction equation Eq. (4) is related to the microscopic diffusivity η with the microscopic dissipation rate $-\mu_0\eta\boldsymbol{j}^2$. On the other hand, the effective dissipation rate in the mean-field energy equation Eq. (62) is given by $-\mu_0(\eta+\eta_t)\overline{\boldsymbol{j}}^2$. Turbulent diffusivity parametrizes a turbulent transport process that transports magnetic energy through advection and reconnection (see Ch. **??** for details regarding reconnection) from the large scale L to the small microscopic scale l at which the energy is dissipated. The energy flux through the turbulent cascade is determined by the large scale and the small scale adjusts to allow for the required dissipation

$$\eta j_l^2 \sim \eta_t \overline{\boldsymbol{j}}^2 \longrightarrow \frac{B_l}{l} \sim \sqrt{R_{\rm m}}\frac{\overline{B}}{L}\ . \tag{64}$$

While in the case of purely hydrodynamic turbulence universal scaling relations such as $v_l \sim l^{1/3}$ exist, this is in general not the case for MHD turbulence. We refer to Ch. **??** for a more detailed discussion of MHD turbulence.

Due to the large magnetic Reynolds numbers in astrophysical systems, the high turbulent diffusivity significantly raises the bar for the creation of large-scale magnetic field.

4.6 Creation of magnetic field: turbulent dynamos

Our main interest here is to understand how fluid motions can support an axisymmetric mean field. Since the total magnetic field $\boldsymbol{B} = \overline{\boldsymbol{B}} + \boldsymbol{B}'$ is in general non-axisymmetric, the maintenance of an axisymmetric mean field is not excluded by Cowling's theorem. However, if the mean-field induction equation is mathematically identical to the 'microscopic' induction equation, Cowling's theorem also rules out the support of an axisymmetric mean field. The effects that change the mathematical form of the mean-field induction equation and therefore allow to circumvent Cowling's anti-dynamo theorem for $\overline{\boldsymbol{B}}$ are the α-effect, the δ-effect and possibly also the β-effect for special cases of anisotropy. We focus the discussion here mainly on the former two.

4.6.1 Generalized Ohm's law

A different way to interpret the turbulent induction effects is by looking at Ohm's law for the mean current. Averaging Ohm's law Eq. (15) leads to

$$\overline{\boldsymbol{j}} = \sigma \left(\overline{E} + \overline{\boldsymbol{v}} \times \overline{\boldsymbol{B}} + \overline{\boldsymbol{\mathcal{E}}} \right) \ . \tag{65}$$

Inserting the expression for the EMF (Eq. [43]) and bringing all terms proportional to $\overline{\boldsymbol{j}}$ (β- and δ-effect) on the left hand side allows to write the mean-field Ohm's law as

$$\overline{\boldsymbol{j}} = \tilde{\boldsymbol{\sigma}} \left(\overline{E} + \overline{\boldsymbol{v}} \times \overline{\boldsymbol{B}} + \boldsymbol{\gamma} \times \overline{\boldsymbol{B}} + \boldsymbol{\alpha} \overline{\boldsymbol{B}} \right) \tag{66}$$

with an anisotropic mean-field conductivity tensor $\tilde{\boldsymbol{\sigma}}$ containing contributions from the molecular conductivity and the β- and δ-effects.

The crucial step in the proof of Cowling's anti-dynamo theorem is the impossibility to maintain a current along the neutral line of the poloidal field even in the presence of a toroidal field. Ohm's law for the mean field, Eq. (66), shows clearly that the α-effect can maintain such a current if a toroidal field is present and therefore allows for the maintenance of an axisymmetric mean field by fluid motions. This is not the only term which potentially has such a property. If we set $\boldsymbol{\alpha} = 0$ on the right-hand side of Eq. (66), the remaining terms would drive currents perpendicular to the mean field. If the conductivity tensor $\tilde{\boldsymbol{\sigma}}$ is sufficiently anisotropic these currents can have again components aligned with the mean field an can therefore also circumvent Cowling's anti-dynamo theorem. The latter is a possible dynamo scenario involving the δ-effect.

4.6.2 α^2-dynamo

The additional induction effect introduced by the α-effect can be most easily understood for isotropic, homogeneous α, which leads in the mean field induction equation (Eq. 42 with Eq. 48) to the additional term

$$\frac{\partial \overline{\boldsymbol{B}}}{\partial t} = \ldots + \boldsymbol{\nabla} \times \left(\alpha \overline{\boldsymbol{B}} \right) = \ldots + \alpha \mu_0 \overline{\boldsymbol{j}} \ . \tag{67}$$

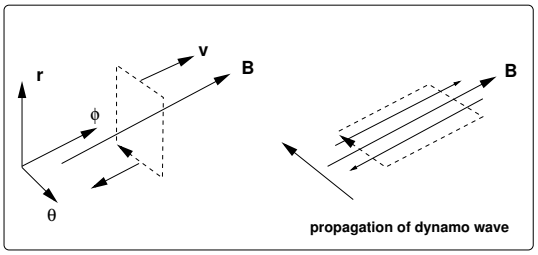

Figure 6: Illustration of dynamo waves in an $\alpha\Omega$-dynamo. The poloidal field (dashed) produced by the α-effect is sheared by the velocity field. The resulting 'new' toroidal field amplifies the original toroidal field on the poleward side and weakens it on the equator ward side. As a result the toroidal field pattern moves poleward in the $-\theta$ direction.

The induced magnetic field is proportional to the mean current. Since the current maintaining a poloidal field is toroidal and the current maintaining a toroidal field is poloidal, this process converts poloidal magnetic field into toroidal field and vise verse. We have therefore the following dynamo scenario:

$$\boldsymbol{B}_t \xrightarrow{\alpha} \boldsymbol{B}_p \xrightarrow{\alpha} \boldsymbol{B}_t \; . \tag{68}$$

Since the α-effect is responsible for the conversion between poloidal and toroidal components in both directions, this type of dynamo is called α^2-dynamo. Inspecting the direction of the currents maintaining the poloidal and toroidal field shows that after completion of a full cycle as indicated in Eq. (68) the magnetic field did not change sign. The α^2-dynamo produces preferably stationary solutions with poloidal and toroidal field of comparable amplitude.

If the α-tensor is anisotropic, the process regenerating $\boldsymbol{B}_t$ from $\boldsymbol{B}_p$ can have a different amplitude than the process regenerating $\boldsymbol{B}_p$ from $\boldsymbol{B}_t$. In that case either $\boldsymbol{B}_t$ or $\boldsymbol{B}_p$ could dominate. The off-diagonal elements of the α-tensor can lead to effects similar to advection effects, i.e. they modify the advection in a way that the effective advection velocity is different for the three field components.

Inserting the expression $\overline{\boldsymbol{\mathcal{E}}} = \alpha \overline{\boldsymbol{B}}$ into the mean-field energy equation Eq. (62) shows that the α-effect sustains the mean field if the mean-field current helicity $\int \overline{\boldsymbol{j}} \cdot \overline{\boldsymbol{B}} \, dV$ has the same sign as α, i.e. the dynamo generated magnetic field is helical. This condition is satisfied because the α-effect induces a magnetic field parallel to the mean current.

4.6.3 $\alpha\Omega$-, $\alpha^2\Omega$-dynamo

We discussed already Sect. 3.7 the effect of differential rotation, leading to a production of toroidal field out of poloidal field. The system Eqs. (35) and (36) is not able to maintain an axisymmetric field since the poloidal field is always decaying. This decay can be prevented in the presence of an α-effect: A dynamo

in which differential rotation is regenerating toroidal field from poloidal field and the α-effect is regenerating poloidal field from toroidal field is called $\alpha\Omega$-dynamo

$$\boldsymbol{B}_t \xrightarrow{\alpha} \boldsymbol{B}_p \xrightarrow{\Omega} \boldsymbol{B}_t \; . \tag{69}$$

The $\alpha\Omega$-dynamo is an approximation that is valid if the Ω-effect is much stronger than the α-effect in producing poloidal field. The mathematical equations describing this type of dynamo are very similar to Eqs. (35) and (36), with η replaced by $\eta + \eta_t$ and an additional term αB in Eq. (36). This type of dynamo leads to magnetic field configurations that are dominated by the toroidal field component. If both the Ω and α-effect contribute significantly to the poloidal field production, the dynamo is called $\alpha^2\Omega$-dynamo.

Unlike the α^2-dynamo, $\alpha\Omega$-dynamos have in general oscillating solutions with magnetic field patterns propagating along lines of constant Ω (Parker-Yoshimura rule: Yoshimura (1975)). The reason for this is illustrated in Fig. (6). In the case of a positive radial gradient in the rotation profile, $\partial\Omega/\partial r$, and positive α this leads to a poleward propagation of the toroidal field pattern. The propagating field pattern of an $\alpha\Omega$-dynamo is very often also referred to as a dynamo wave .

In the case of an $\alpha\Omega$ dynamo the primary energy source for the mean field is the work done against the Lorentz force (second term on the right-hand side of Eq. [62]).

4.6.4 $\Omega \times J$ dynamo

The δ-effect in the mean-field expansion Eq. (48) is also referred to as $\Omega \times J$-effect for obvious reasons. It leads to a field regeneration of the form

$$\frac{\partial \overline{\boldsymbol{B}}}{\partial t} = \boldsymbol{\nabla} \times [\delta \times (\boldsymbol{\nabla} \times \overline{\boldsymbol{B}})] \sim \boldsymbol{\nabla} \times (\Omega \times \overline{\boldsymbol{j}}) \sim \frac{\partial \overline{\boldsymbol{j}}}{\partial z} \tag{70}$$

The currents of a poloidal field are toroidal and therefore also $\partial\overline{\boldsymbol{j}}/\partial z$ is toroidal. The currents of a toroidal field are poloidal and therefore also $\partial\overline{\boldsymbol{j}}/\partial z$ is poloidal in that case. Similar to the α-effect, the δ-effect can convert toroidal into poloidal field and vice verse. However, unlike the α-effect a δ^2 dynamo is not possible. This becomes evident from the mean-field energy equation Eq. (62) since in the case of the δ-effect

$$\overline{\boldsymbol{j}} \cdot \overline{\mathcal{E}} = \overline{\boldsymbol{j}} \cdot (\boldsymbol{\delta} \times \overline{\boldsymbol{j}}) = 0 \; . \tag{71}$$

This does not rule out dynamos such as a $\delta\Omega$ dynamo, in which the Ω-effects pumps energy into the mean field (second term on the right hand side of Eq. (62)), while the δ-effect is required to reproduce poloidal from toroidal field (change of topology).

We want to mention that the δ-effect is controversial since not all approaches used to calculate the mean-field transport coefficients lead to a δ-effect. Also in most astrophysical systems the α-effect is normally the dominant mechanism.

4.7 Dynamos and magnetic helicity

The magnetic helicity is defined as the volume integral of the product between the magnetic field $\boldsymbol{B}$ and its vector potential $\boldsymbol{A}$

$$H_m = \int \boldsymbol{A} \cdot \boldsymbol{B} \, dV \ . \tag{72}$$

The magnetic helicity is an integral measure of magnetic field topology. Since the vector potential $\boldsymbol{A}$ allows for some gauge freedom, also magnetic helicity reflects that ambiguity. It is nevertheless a very helpful quantity since it is conserved under ideal MHD. We refer here to Ch. **??** for a more detailed discussion of magnetic helicity and its topological meaning.

Assuming that there are no helicity fluxes across the domain boundaries, the induction equations provides a conservation law for the magnetic helicity of the form

$$\frac{d}{dt} \int \boldsymbol{A} \cdot \boldsymbol{B} \, dV = -2\mu_0 \, \eta \int \boldsymbol{j} \cdot \boldsymbol{B} \, dV \ , \tag{73}$$

where the property $\int \boldsymbol{j} \cdot \boldsymbol{B} \, dV$ is the current helicity of the magnetic field. Magnetic helicity is strictly conserved for ideal MHD. For astrophysical systems with very large magnetic Reynolds numbers it can evolve only on a very slow resistive time scale. In this case helicity conservation can be still a significant constraint as we see in Sect. 5.2.

Deriving a similar equation for the mean field and subtracting that equation from Eq. (73) allows us to split the helicity evolution into the large and small-scale parts leading to

$$\frac{d}{dt} \int \overline{\boldsymbol{A}} \cdot \overline{\boldsymbol{B}} \, dV = +2 \int \overline{\boldsymbol{\mathcal{E}}} \cdot \overline{\boldsymbol{B}} \, dV - 2\mu_0 \, \eta \int \overline{\boldsymbol{j}} \cdot \overline{\boldsymbol{B}} \, dV \tag{74}$$

$$\frac{d}{dt} \int \overline{\boldsymbol{A}' \cdot \boldsymbol{B}'} \, dV = -2 \int \overline{\boldsymbol{\mathcal{E}}} \cdot \overline{\boldsymbol{B}} \, dV - 2\mu_0 \, \eta \int \overline{\boldsymbol{j}' \cdot \boldsymbol{B}'} \, dV \ . \tag{75}$$

Inserting the expression $\overline{\boldsymbol{\mathcal{E}}} = \alpha \overline{\boldsymbol{B}}$ shows that the α-effect induces on the large-scale magnetic helicity with the same sign of the α effect, while the small-scale helicity has the opposite sign. In the case of stationarity, which is only achieved on a slow resistive time scale, the same also applies to the current helicity. We show later that the accumulation of current helicity on the small scale can lead to a significant reduction of the α-effect.

4.8 General comments on large-scale turbulent dynamos

All large-scale turbulent dynamo scenarios discussed here contain at least one process (either α or δ) related to a pseudo vector or tensor. According to Eq. (50) this requires a preferred direction expressed by a pseudo vector, which is rotation ($\boldsymbol{\Omega}$) in most astrophysical systems (also shear flows could define such a pseudo vector through $\boldsymbol{\nabla} \times \overline{\boldsymbol{v}}$). For a dynamo of the type α^2 or $\alpha^2\Omega$ rotation alone is not sufficient, since the α effect requires an additional symmetry direction to

exist. In most cases this additional preferred direction is stratification, but also the influence of boundary conditions can be sufficient: turbulence resulting from isotropic forcing and rotation has an α-effect near boundaries, since the normal vector to the boundary introduces a preferred direction in the velocity field. In the case of the geodynamo such boundary effects at the core-mantle boundary are crucial since the system is only weakly stratified (incompressible).

The turbulent induction effects that enable large-scale dynamo action do not necessarily have to convert energy to maintain the mean field. In the presence of strong differential rotation most of the energy conversion is done through the large-scale shear flow,and the role of the α- or δ-effect is reduced to changing the field topology (production of poloidal field from toroidal field).

The mean-field dynamos we discussed here are all fast dynamos. Even though the α- and β-effect require reconnection and are therefore indirectly dependent on a microscopic η, the expressions we derived for α in Eq. (59) do not contain η explicitly and are independent of $R_{\rm m}$ (within the limits of the approximations we made). We show in Sect. 5.2 that under certain conditions this conclusion does not hold and α can become asymptotically limited by the microscopic value of η.

Another more fundamental question in dynamo theory is related to the linear homogeneous structure of the induction equation, which means that $\boldsymbol{B} = \boldsymbol{0}$ is always a valid solution. Having a dynamo means that the solution $\boldsymbol{B} = \boldsymbol{0}$ is unstable and any small perturbation leads to an exponential growth (linear kinematic phase) until non-linear feedbacks through the Lorentz force become important. We want to mention that there are also other processes that can produce large-scale fields if the more general form of Ohm's law Eq. (14) is used. Keeping the electron pressure term and re-deriving the induction equation leads to an additional term $\sim \boldsymbol{\nabla} n_e \times \boldsymbol{\nabla} p_e$. Unlike the other terms that only contribute if there is already a magnetic field present, this term is a real source provided that the gradients of electron density and temperature are not parallel (e.g. ionization fronts in an inhomogeneous medium). However, these fields are very weak and additional amplification through dynamo processes is required nevertheless.

5 Limitations of mean-field approximation, 3D simulations

5.1 Comments on general applicability

We computed expressions for the dynamo coefficients in Sect. 4.3 by using the second order correlation approximation (SOCA). In the case of large magnetic Reynolds numbers, which is typical for stellar convection zones, this approximation is only justified when the Strouhal number $S = v\tau_c/l_c$ is much smaller than unity. Typical values for convection are close to unity since the basic mixing-length relation $l_c \sim H_p \sim v\,\tau_c$ holds. Therefore the justification of this approach is at best marginal. Nevertheless, the expressions derived from SOCA Eq. (55)

give a reasonable agreement when tested in numerical simulations (Käpylä et al. (2006)), which might indicate that the applicability of the expressions derived from SOCA might go beyond the regime with $S = v\tau_c/l_c \ll 1$. We emphasize that the expressions Eq. (55) can remain valid even if $B' \gg \overline{B}$ provided that $\boldsymbol{v}'$ correlates only weakly with $\boldsymbol{\nabla} \times (\boldsymbol{v}' \times \boldsymbol{B}')$.

The constraints on the general applicability of the mathematical form of the mean-field expansion Eq. (48) are less severe, since Eq. (48) follows from very general symmetry principles. A requirement for the fast convergence of the spatial part of this expansion is a sufficient scale separation, which has to be tested in a given application. If locality in time is not justified, terms such as $\overline{\boldsymbol{\mathcal{E}}} \sim \alpha \overline{\boldsymbol{B}}$ have to be replaced by terms of the form

$$\overline{\boldsymbol{\mathcal{E}}} \sim \int_{-\infty}^{t} \alpha(t, t') \overline{\boldsymbol{B}}(t') dt' \tag{76}$$

An alternative (equivalent) approach would be solving an evolution equation for $\overline{\boldsymbol{\mathcal{E}}}$.

In the case of the solar dynamo we have $\tau_c \sim 10\,\text{days}$ deep in the convective envelope while the mean field is evolving on a times scale of several years. The scale separation in time is about two orders of magnitude and well justified. Convective cells at the base of the convection have a length scale comparable to the density scale height $l_c \sim 10^8\,\text{m} \sim 0.15 R_\odot$. The scale separation in the length scales is only marginally justified. Therefore higher order derivatives of the mean field could be required (leading to hyper-diffusive behavior). In the case of the geodynamo the scale separation in length scales is comparable to the solar dynamo, but the mean field shows variability on the times scale τ_c itself. Mean-field theory in the form of Eq. (48) is here only helpful for understanding the structure of the temporally averaged field (averaging the dipole moment for 10^3 to 10^4 years removes most of the variability except reversals).

One of the biggest limitations is in general that it is not easy to compute the mean-field coefficients $\alpha, \ldots, \delta$ from first principles. The first problem is that one needs a velocity field $\boldsymbol{v}'$, the second problem is that one has to solve Eq. (44) in order to be able to compute the electromotive force $\overline{\boldsymbol{\mathcal{E}}}$ (Eq. [43]). We presented a very crude approach for the second step in Sect. 4.3. Approaches that combine both steps use in general a spectral representation and compute the anisotropies and inhomogeneities resulting from rotation and stratification from the Navier-Stokes equations using a quasi-linear approach. Expressions for the dynamo coefficients obtained this way have been compared to numerical simulations (see below) and show in general a qualitative agreement. Differences are caused by both the limitation of the mean-field approach and limitations of numerical simulations. More details on different ways to compute dynamo coefficients can be found in Rädler & Stepanov (2006), Rädler & Rheinhardt (2006) and Rüdiger & Hollerbach (2004).

5.2 Non-kinematic effects

A much more detailed summary of non-linear dynamo theory and advances in this field can be found in Brandenburg & Subramanian (2005). In Sect. 4 we followed the kinematic approach. We assumed that a turbulent velocity field $\boldsymbol{v}'$ was given and focused only on solving the induction equation. Since this equation is linear, solutions show either an exponential decay or growth. The kinematic approach is useful to understand the onset of dynamo action, but leaves out the interesting question of saturation of a dynamo. This can be addressed only if the Lorentz force is considered in the Navier-Stokes equation, which requires in general solving the full system of the MHD-equations. The Lorentz force modifies the small scale flows leading to turbulent induction effects as well as the large-scale mean flows (e.g., differential rotation). The influence of the Lorentz force on the mean flows is referred to very often as macroscopic feedback (also Malkus-Proctor effect; Malkus & Proctor (1975)). The components of the Lorentz force that change the large-scale flows are given by

$$\overline{\boldsymbol{j} \times \boldsymbol{B}} = \overline{\boldsymbol{j}} \times \overline{\boldsymbol{B}} + \overline{\boldsymbol{j}' \times \boldsymbol{B}'} \; . \tag{77}$$

While the first term on the right-hand side is directly accessible in a mean field model, the second term requires the fluctuating fields which are in general not known. Most of the non-linear models with macroscopic feedback such as the models by Covas et al. (2000), Bushby (2005) and Rempel (2006) do only consider the contribution from the mean field (first term).

The microscopic feedback on the small-scale motions has been included through ad-hoc quenching parametrizations such as

$$\alpha = \frac{\alpha_{\mathrm{k}}}{1 + \left(B/B_{\mathrm{eq}}\right)^2} \; . \tag{78}$$

Here α_{k} denotes the kinematic expression from Eq. (59) and B_{eq} the equipartition field strength given by $\frac{1}{2}\varrho v_{\mathrm{rms}}^2 = \frac{1}{2\mu_0} B_{\mathrm{eq}}^2$. The rationale behind this expression is that the small-scale motions are reduced in amplitude once the magnetic energy density is similar to the kinetic energy density of turbulent motions.

Vainshtein & Cattaneo (1992) and Cattaneo & Hughes (1996) suggested that this expression has to be modified to

$$\alpha = \frac{\alpha_{\mathrm{k}}}{1 + R_{\mathrm{m}} \left(B/B_{\mathrm{eq}}\right)^2} \; , \tag{79}$$

which is referred to also as catastrophic α-quenching due to the large value of R_{m} in astrophysical systems, which would basically rule out an α-effect for any field strength of interest.

The saturation of the α-effect is closely related to the evolution of magnetic helicity. Pouquet et al. (1976) showed that the small-scale current helicity leads to a magnetic correction of the α-effect:

$$\alpha = -\frac{1}{3}\tau_c \left(\overline{\boldsymbol{\omega}' \cdot \boldsymbol{v}'} - \frac{1}{\varrho} \overline{\boldsymbol{j}' \cdot \boldsymbol{B}'} \right) \; . \tag{80}$$

The buildup of small-scale helicity according to Eq. (75) creates a magnetic α-effect (second term on right-hand side of Eq. [80]) that offsets the kinematic α-effect (first term). Since we do not have observational evidence for catastrophic quenching in astrophysical dynamos it has been suggested by Brandenburg & Sandin (2004) that small scale helicity losses might alleviate the catastrophic quenching. In the case of the Sun there is observational evidence for losses of negative helicity in the northern and positive helicity in the southern hemisphere.

5.3 3D dynamo simulations

With the significant advance in computing power 3D dynamo simulations solving the full set of MHD equations have become a very powerful tool in dynamo theory. It remains, however, a significant challenge with varying success for different objects. The main difficulty in simulating large-scale dynamos results from the fact that it is required to capture the large scale and at the same time the significantly smaller scales of the turbulence. In a local turbulence simulation the largest scales are typically not far above the energy carrying scales of the turbulence, which are for the solar dynamo at least one order of magnitude smaller than the global scale of the system (solar radius). Furthermore, large-scale dynamos evolve typically on time scales much longer than the overturning time scale of turbulent motions (e.g., for the solar dynamo we have $P_{\rm cyc} \approx 22\,{\rm years} \approx 8000\,{\rm days}$ and $\tau_c \approx 10\,{\rm days}$). This makes studying a large-scale dynamo much more challenging than a local simulation of turbulence, which is typically run only over a few overturning time scales. A further complication comes from the fact that most astrophysical systems (except galaxies) have a very low magnetic Prandtl number, meaning $R_{\rm m} \ll R_{\rm e}$. Since dynamo action requires to exceed a minimum $R_{\rm m}$, relatively large values of $R_{\rm e}$ are required in general (this problem is often avoided by forcing the magnetic Prandtl number to be close to unity). Due to these difficulties, large-scale dynamos (or at least some of the ingredients) have been studied using also more local approaches as we briefly outline in the Sect. 5.3.1.

5.3.1 Local simulations

Local simulations place a computational domain significantly smaller that the full system (e.g., 10% of the size of the star) at a given latitude. The latitude is defined through the orientation of the axis of rotation with respect to the vertical direction that defines the direction of gravity. Since simulation cannot include the density contrast of about 10^6 in the solar convection zone, also only a fraction of the radial extent of the convection zone is covered. The depth location of the box is indirectly imposed through the Coriolis number (defined as $Co = 2\Omega\tau_c$) measuring the influence of rotation (in the solar convection zone the Coriolis number is increasing from less than 1 at the surface to about 10 at the base of the convection zone). This approach is also called f-plane approximation.

A setup like this allows the study of ingredients of a large-scale dynamo, such as the α and γ-effect (turbulent pumping), without addressing the large scale. As a consequence local simulations are not necessarily a dynamo (except for small-scale dynamo action) but rather a magneto-convection simulation in which a large-scale mean field is imposed to 'measure' dynamo coefficients. Ossendrijver et al. (2001, 2002) and Käpylä et al. (2006) computed dynamo coefficients as function of latitude and Coriolis number (influence of rotation, mainly depth dependent) and found a rather good correspondence between the numerically computed dynamo coefficients and those computed from the second order correlation approximation Eq. (55) in the case of moderate rotation and a qualitative agreement in the case of fast rotation.

5.3.2 Global simulations

Despite the computing power available today, global simulations of dynamos remain very challenging. While self-consistent dynamo models for the geodynamo have been presented first about a decade ago (Glatzmaier & Roberts (1995), building upon earlier work of Glatzmaier & Gilman (1982), Gilman (1983) and Glatzmaier (1984)), a self-consistent dynamo model for the solar dynamo has not been achieved so far. In the case of the geodynamo the relatively low magnetic Reynolds number of the order of a few 100 works in favor of numerical simulations, since it is possible to resolve all relevant magnetic scales of the dynamo. The flow Reynolds number is however still significantly larger, which requires subgrid-scale modeling for the velocity field. As long as the unresolved scales in the velocity field only exhibit a diffusive behavior for the magnetic field it is possible to capture all relevant induction effects in a 3D simulation. For a summary of the main dynamo mechanism of the geodynamo see Olson et al. (1999).

Unlike in the case of the geodynamo, numerical models for the solar dynamo are far away from resolving all relevant magnetic scales. Current simulations of the global solar convection are of the order of 1000^3 in grid size and can be run a few years of real time. Expanding the time covered by at least a factor of 10 (to cover a cycle) and increasing the resolution by a factor of 3 would increase the demand of computing power by roughly a factor of 10^3. An additional major problem in 3D simulations of the solar dynamo is modeling the transition layer at the base of the solar convection zone (tachocline), which shows strong radial shear in the differential rotation and most likely plays a key role in the dynamo process. The transition toward the more stable radiative interior of the Sun introduces time scales far beyond the convective times scales governing the convection zone of the Sun.

Early work of Gilman (1983) showed cyclic dynamos in spherical 3D simulations; however, more turbulent simulations at higher resolution do not yield periodic solutions for solar parameters ((Brun et al. 2004), (Browning et al. 2006)). Nevertheless there is significant progress in understanding important ingredients of the dynamo process with increasing detail. For a review of dynamics of the solar convection zone from 3D simulations we refer to Miesch (2005). Unfortu-

nately, knowledge of the basic dynamo ingredients is not sufficient to determine the primary dynamo process, since all these ingredients (except differential rotation) have an uncertain amplitude and spatial distribution within the solar convection zone. This leads to quite a variety of different dynamo scenarios as summarized by Ossendrijver (2003) and Charbonneau (2005).

References

Backus, G. 1958, Annals of Physics, 4, 372

Braginskii, S. 1964, Sov. Phys., 20, 1462

Brandenburg, A. & Sandin, C. 2004, A&A , 427, 13

Brandenburg, A. & Subramanian, K. 2005, Physics Reports , 417, 1

Browning, M. K., Miesch, M. S., Brun, A. S., & Toomre, J. 2006, ApJL , 648, L157

Brun, A. S., Miesch, M. S., & Toomre, J. 2004, ApJ , 614, 1073

Bullard, E. C. & Gellman, H. 1954, Phil. Trans. R. Soc. A, 247, 213

Bushby, P. J. 2005, Astronomische Nachrichten, 326, 218

Cattaneo, F. 1999, ApJL , 515, L39

Cattaneo, F. & Hughes, D. W. 1996, Phys. Rev. E , 54, 4532

—. 2001, Astronomy and Geophysics, 42, 18

Charbonneau, P. 2005, Living Reviews in Solar Physics, 2, 2

Choudhuri, A. R., Schüssler, M., & Dikpati, M. 1995, A&A , 303, L29

Covas, E., Tavakol, R., Moss, D., & Tworkowski, A. 2000, A&A , 360, L21

Cowling, T. G. 1933, Mon. Not. R. Astron. Soc. , 94, 39

Davidson, P. A. 2001, An introduction to magnetohydrodynamics (An introduction to magnetohydrodynamics, Cambridge, UK: Cambridge University Press, 2001 xviii, 431 p. Cambridge texts in applied mathematics, ISBN 0521791499)

Dikpati, M. & Charbonneau, P. 1999, ApJ , 518, 508

Elsasser, W. M. 1946, Physical Review, 69, 106

Gailitis, A. 1970, Magnetohydrodynamics, 6, 14

Gilman, P. A. 1983, ApJS , 53, 243

Glatzmaier, G. A. 1984, Journal of Computational Physics, 55, 461

Glatzmaier, G. A. & Gilman, P. A. 1982, ApJ , 256, 316

Glatzmaier, G. A. & Roberts, P. H. 1995, Nature , 377, 203

Herzenberg, A. 1958, Phil. Trans. R. Soc. A, 250, 543

Käpylä, P. J., Korpi, M. J., Ossendrijver, M., & Stix, M. 2006, A&A , 455, 401

Larmor, J. 1919, Br. Assoc. Adv. Sci. Rep., 159

Malkus, W. V. R. & Proctor, M. R. E. 1975, Journal of Fluid Mechanics, 67, 417

Miesch, M. S. 2005, Living Reviews in Solar Physics, 2, 1

Moffatt, H. K. 1978, Magnetic field generation in electrically conducting fluids (Cambridge University Press)

Olson, P., Christensen, U., & Glatzmaier, G. A. 1999, jgr, 104, 10383

Ossendrijver, M. 2003, Astron. Astrophys. Rev., 11, 287

Ossendrijver, M., Stix, M., & Brandenburg, A. 2001, A&A , 376, 713

Ossendrijver, M., Stix, M., Brandenburg, A., & Rüdiger, G. 2002, A&A , 394, 735

Parker, E. N. 1955, ApJ , 122, 293

—. 1979, Cosmical magnetic fields: Their origin and their activity (Oxford, Clarendon Press; New York, Oxford University Press, 1979, 858 p.)

—. 2007, Conversations on Electric and Magnetic Fields in the Cosmos (Conversations on Electric and Magnetic Fields in the Cosmos, by Eugene N. Parker. ISBN-10 0-691-12840-5 (HB); ISBN-13 978-0-691-12840-5 (HB). Published by Princeton University Press, Princeton, NJ USA, 2007.)

Pouquet, A., Frisch, U., & Leorat, J. 1976, Journal of Fluid Mechanics, 77, 321

Proctor, M. R. E. & Gilbert, A. D. 1995, Lectures on Solar and Planetary Dynamos (Lectures on Solar and Planetary Dynamos, Edited by M. R. E. Proctor and A. D. Gilbert, pp. 389. ISBN 0521461421. Cambridge, UK: Cambridge University Press, January 1995.)

Rädler, K.-H. 1980, Astronomische Nachrichten, 301, 101

Rädler, K.-H. & Rheinhardt, M. 2006, ArXiv Astrophysics e-prints

Rädler, K.-H. & Stepanov, R. 2006, Phys. Rev. E , 73, 056311

Rempel, M. 2006, ApJ , 647, 662

Rüdiger, G. & Hollerbach, R. 2004, The Magnetic Universe: Geophysical and Astrophysical Dynamo Theory (ISBN 3-527-40409-0. Wiley-VCH)

Schrijver, C. J. & Zwaan, C. 2000, Solar and Stellar Magnetic Activity (Solar and stellar magnetic activity / Carolus J. Schrijver, Cornelius Zwaan. New York : Cambridge University Press, 2000. (Cambridge astrophysics series ; 34))

Shu, F. H. 1992, Physics of Astrophysics, Vol. II (Physics of Astrophysics, Vol. II, by Frank H. Shu. Published by University Science Books, ISBN 0-935702-65-2, 476pp, 1992.)

Steenbeck, M., Krause, F., & Rädler, K. H. 1966, Zeitschrift Naturforschung Teil A, 21, 369

Stix, M. 2004, The sun : an introduction (The sun : an introduction, 2nd ed., by Michael Stix. Astronomy and astrophysics library, Berlin: Springer, 2004. ISBN: 3540207414)

Vainshtein, S. I. & Cattaneo, F. 1992, ApJ , 393, 165

Vögler, A. & Schüssler, M. 2007, A&A , 465, L43

Yoshimura, H. 1975, ApJS , 29, 467